Design Data for Radial-Waveguide Circulators Using Partial-Height Ferrite Resonators

JOSEPH HELSZAJN, MEMBER, IEEE, AND FRANCIS C. TAN

Abstract—**This paper derives the eigennetworks of radial-waveguide circulators using partial-height ferrite resonators with $n=2$ Chebyshev characteristics. To obtain a Chebyshev response with such junctions it is necessary to establish the proper phase angles and admittance levels of the three eigennetworks of the device. This paper derives the phase angles for the eigennetworks but relies on experiments to establish the admittance levels. The configurations dealt with include the standard circulators using either half-wave-long ferrite resonators open circuited (OC) at both ends or coupled quarter-wave-long ferrite resonators OC at one end and short circuited (SC) at the other. It also includes the design of a new single quarter-wave-long version, which is likely to replace the two more conventional arrangements in common usage. It is observed that the eigennetworks of any one of the geometries is sufficient to characterize the other two.**

INTRODUCTION

THE MOST USEFUL of the experimental H-plane waveguide circulators with equal-ripple Chebyshev characteristics uses partial-height ferrite geometries between metal transformer plates. Experimental constructions reported so far include coupled quarter-wave-long ferrite disks open circuited (OC) at one end and short circuited (SC) at the other [1], single half-wave-long geometries OC at both ends [2], and single cylinders three or five quarter-wave-long OC at one end and SC at the other [3], [4]. An equal-ripple Chebyshev characteristic may be obtained with such configurations by establishing the proper phase angles and admittance levels of the three eigennetworks of the junction. The theory of these circulators is not yet fully understood but their mode nomenclature has now been identified as axial ones associated with the hybrid $HE_{11\delta}$ mode on a dielectric waveguide [4].

To adjust these and other circulators requires a 120° phase difference between the reflection coefficients of the three different ways it is possible to simultaneously excite the three rectangular waveguides which will give identical reflection coefficients at each port. One of these excitations corresponds to in-phase fields at the three ports, while the other two require counter-rotating field patterns. These latter field patterns propagate along the magnetized ferrite section with different propagation constants. The former field pattern does not couple to the circular waveguide but is reflected at the junction of the device. Excitation of a single port establishes all three field patterns within the junction. The purpose of this paper is to give the eigennetworks for these three excitations for some partial-height ferrite geometries.

The two standard configurations considered in this paper are depicted in Fig. 1(a) and (b). The first consists of a single ferrite cylinder in a circular radial cavity connected to three rectangular waveguides at the characteristic planes of the junction [5]. These planes have the property of uniquely defining the input terminals of the radial admittance transformer of the quarter-wave coupled device. The second geometry is similar to the first except that it uses two ferrite disks instead of one cylinder. It is found that the two have identical eigennetworks so that a single set of physical variables can be used to describe either of them. This is done by relating the phase angles of their eigennetworks through the method of images and relying on experiment for the admittance levels. These eigennetworks involve ideal transformers to represent the coupling of the counter-rotating modes into the ferrite disks. The method of images also leads to the new single-disk geometry depicted in Fig. 1(c), which is described by the same set of physical variables as the former two,

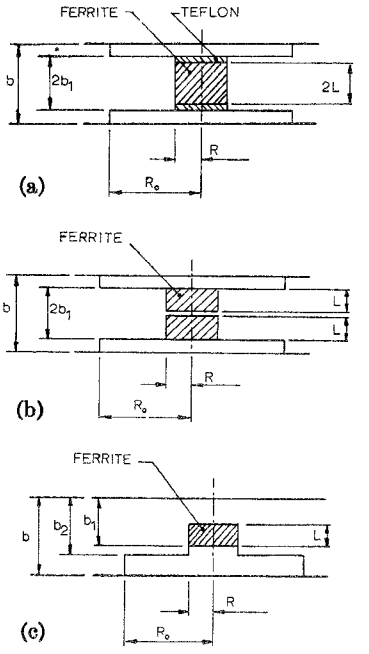

Fig. 1. (a) Schematic of single-cylinder resonator radial waveguide circulator. (b) Schematic of two open-ferrite-disk resonator radial waveguide circulators. (c) Schematic of single open-ferrite resonator radial waveguide circulator.

Manuscript received September 24, 1973; revised February 1, 1974, May 6, 1974, August 8, 1974, and September 13, 1974.

The authors are with the Department of Electrical and Electronic Engineering, Heriot-Watt University, Edinburgh, Scotland.

except that its junction susceptance slope parameter is twice that of the other two geometries. This means that a single set of physical variables may be used to characterize all three partial-height ferrite geometries discussed in this text and that measurements on any one of them is sufficient to characterize the others. It is further observed that it is possible to obtain essentially similar performance with any one of them.

However, a shortcoming of the first two geometries is that although it is not difficult to establish the phase angles of the eigennetworks for an ideal circulator design, it is less easy to obtain the admittance levels for the equal-ripple Chebyshev one. This is due to the fact that the spacing between the cylinder and the waveguide walls and spacing between the two ferrite disks not only determine the phase angle of the in-phase eigennetwork, but also the turns ratio of the ideal transformers used to represent the coupling of the counter-rotating modes into the ferrite disks, and the admittance of the radial admittance transformer. This difficulty does not arise with the third geometry in Fig. 1(c) where each independent variable may be established separately provided an additional independent variable in the form of a thin metal post is introduced through the center of the junction to adjust the phase angle of the in-phase eigennetwork without perturbing the counter-rotating ones.

The paper includes the design of single-disk and coupled-disk circulators with similar overall frequency responses using the approach derived in this text. However, the single-disk geometry leads to a wider range of characteristics than is possible with other types where more than one electrical variable is influenced by a single physical one and is likely to replace them.

IMAGE PLANES OF PARTIAL-HEIGHT FERRITE CIRCULATORS

Circulators using partial-height geometries are related to the original turnstile junction [2], [18]. Fig. 1(a) and (b) illustrate the two standard commonly used geometries, and Fig. 1(c) depicts a further one which is related to the first two through the method of images. The frequencies of all these circulators are determined by open dielectric resonances of the dielectric waveguide mode for which a mode chart is given later in the text.

The path lengths of the three geometries in Fig. 2(a)–(c) may all be related to quarter-wave-long SC transmission lines by the method of images. This is done by introducing symmetry planes into the two configurations in Fig. 2(a) and (b) and relating them to that in Fig. 2(c). The signs of the field polarities of the two images can be assigned by noting that the tangential electric field is zero at the image plane (plane of symmetry). It is immediately observed that it is possible to introduce a conducting plane at the plane of symmetry of the half-wave-long geometry shown in Fig. 2(a), since the tangential electric field is zero at that plane. The field polarities are illustrated in Fig. 2. The symmetry plane and the field polarities in the case of the geometry in Fig. 1(b) are indicated in Fig. 2(b). The fields are oppositely orientated in the two image disks in Fig. 2(a) and (b) as required from the Faraday rotation description, since propagation is otherwise in the opposite direction along the two disks.

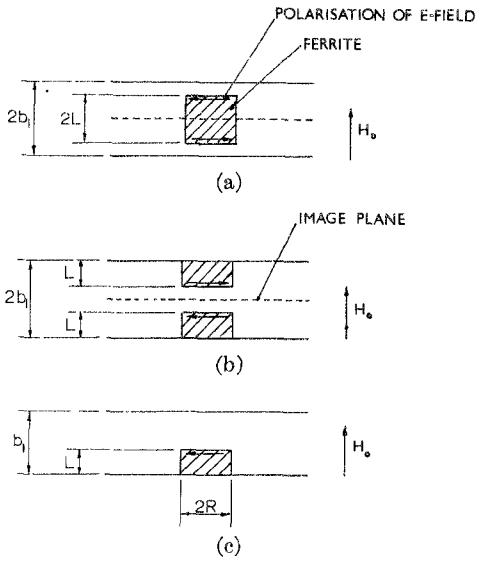

Fig. 2. Image relations between commercial waveguide circulators.

The in-phase mode is determined by the spacing between the OC faces of the ferrite disks and the waveguide or image walls of the junction.

This result indicates that a single set of radial dimensions can be used to describe all three geometries in Fig. 1(a)–(c) provided the spacing between the ferrite disk is dimensioned with respect to the waveguide wall in Fig. 1(c) and with respect to the image planes in the cases of Fig. 1(a) and (b). The equivalence between these geometries also applies to the frequency shift of the open dielectric resonator due to the proximity the waveguide wall or the image plane, as the case may be.

The choice of any single geometry is therefore determined by historical development but the geometry illustrated in Fig. 1(c) appears to offer the most promise.

WAVEGUIDE CIRCULATOR BOUNDARY CONDITIONS

The circulator boundary conditions in the case of the waveguide circulator are best stated in terms of the coefficient of the scattering matrix. These latter parameters are known once the eigenvalues of the $\bar{S}$ matrix are obtained. The problem therefore reduces to that of finding the eigenvalues of the $\bar{S}$ matrix in terms of the EM problem. These may be obtained one at a time by making use of the symmetry properties of the $\bar{S}$ matrix [13], [14].

The scattering matrix of the 3-port junction is given in the usual way by

$$\bar{S} = \begin{bmatrix} S_{11} & S_{12} & S_{13} \\ S_{13} & S_{11} & S_{12} \\ S_{12} & S_{13} & S_{11} \end{bmatrix}. \tag{1}$$

The entries of the $\bar{S}$ matrix are [6], [18]

$$3S_{11} = s_0 + s_{+1} + s_{-1} \tag{2}$$

$$3S_{12} = s_0 + s_{+1} \exp(j120) + s_{-1} \exp(-j120) \tag{3}$$

$$3S_{13} = s_0 + s_{+1} \exp(-j120) + s_{-1} \exp(j120). \tag{4}$$

If the eigenvalues can be calculated or measured, the amplitude and phase of the scattering elements can be determined. One way in which the eigenvalues may be obtained one at a time is to obtain the reflection coefficient at any port with incident fields proportional to the three eigenvectors of the junction.

The three eigennetworks for the junctions considered here are shown in Fig. 3(a) and (b). The ones in Fig. 3(a) apply to the first two geometries, and that in Fig. 3(b) to the single-disk version. The $n = 0$ mode has a pole at the origin while all other modes have zeros there. The equivalent-circuit circuit for the $n = 0$ mode is therefore an OC network and the ones for $n = \pm 1$ are SC networks. The ideal transformers represent the coupling of the $n \pm 1$ modes into the ferrite disks.

Maximum power transfer through the reciprocal junction occurs when $s_{+1} = s_{-1} = s_1$ and $s_0 = -s_1$. The object of this paper is to establish this condition as a preliminary to design.

MAXIMUM POWER TRANSFER IN A 3-PORT JUNCTION WITH FERRITE DISKS

The maximum power-transfer condition in a 3-port junction is obtained by forming the reflection coefficient of the device.

The reflection coefficient for a reciprocal junction is

$$S_{11} = \frac{s_0 + 2s_1}{3}. \tag{5}$$

Maximum power transfer through the junction occurs when

$$s_1 = -s_0. \tag{6}$$

This requires the following relation between the angles of the eigenvalues:

$$\Theta_0 = \Theta_1 + 90°. \tag{7}$$

The boundary condition for the counter-rotating modes is $s_1 = +1$. This requires $H_\theta = 0$ at $r = R$ which will be shown to coincide with

$$(kR)_{11} = 1.84. \tag{8}$$

The boundary condition for the in-phase mode is $s_0 = -1$. This is obtained by setting $E_z = 0$ at $r = R$. This will be shown to coincide with

$$(k_e R)_{01} = 2.405. \tag{9}$$

The previous two conditions may be satisfied simultaneously by noting that the first boundary condition is primarily determined by L and is essentially independent of R. This means that L may be used as an independent variable to satisfy the first boundary condition and R, and the filling factor L/b_1 may be used to satisfy the second one.

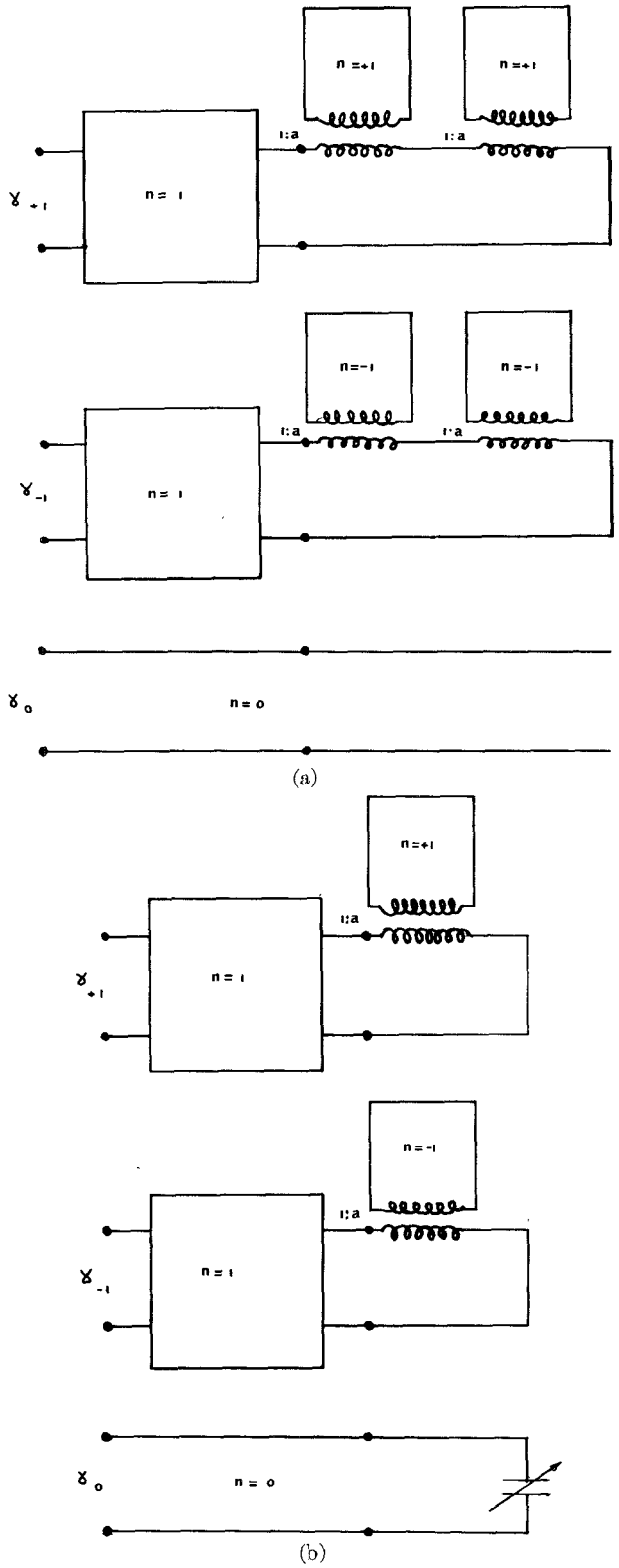

Fig. 3. (a) Eigennetworks of coupled disks and single-cylinder waveguide circulators. (b) Eigennetworks of single-disk waveguide circulator.

If the boundary conditions for maximum power transfer are applied at the input terminals of a quarter-wave

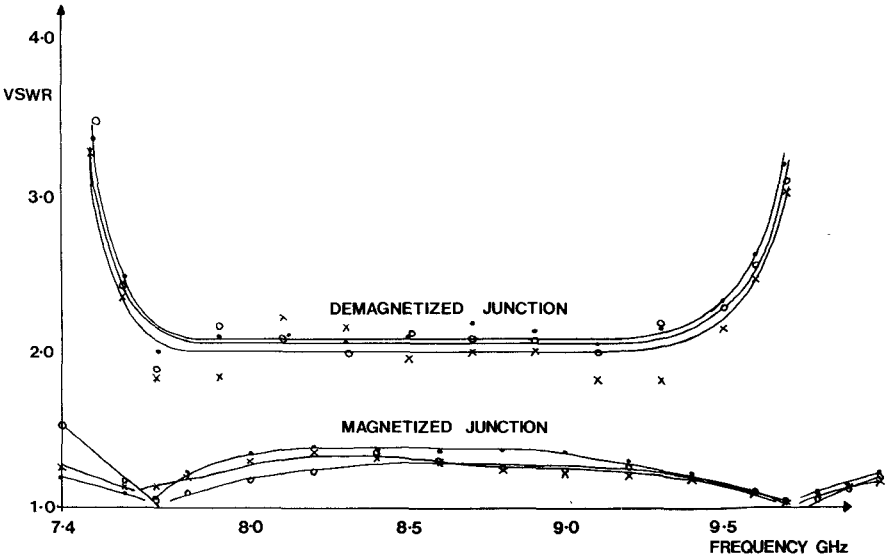

Fig. 4. Frequency response of magnetized and demagnetized junction.

coupled circulator, the phase angles of s_0 and s_1 at the ferrite terminals are shifted by 180°. The new boundary conditions at these terminals therefore become $s_0 = 1$ and $s_1 = -1$ instead of $s_0 = -1$ and $s = 1$.

The first boundary condition gives $E_z = 0$ at $r = R_0$ for which

$$B_1 J_1(k_0 R_0) + C_1 Y_1(k_0 R_0) = 0. \tag{10}$$

The second boundary condition requires that $H_\theta = 0$ at $r = R_0$, which gives

$$B_0 J_0'(k_0 R_0) + C_0 Y_0'(k_0 R_0) = 0. \tag{11}$$

In a uniform transmission line these latter two conditions can be established simultaneously with those given by (8) and (9) which apply at the ferrite radius. However, in a nonuniform line such as a radial one if the two equations for s_1 are satisfied at the two sets of terminals, it is not possible to satisfy s_0 simultaneously at the same terminals. The two boundary conditions for s_0 give lower and upper bounds on L/b_1.

An important property of 3-port junctions is that the plane at which $s_1 = -1$ coincides with the definition of characteristic planes in such junctions. This property will be used in this text to satisfy this boundary condition. It is satisfied from (10) when

$$k_0 R_0 = 3.45. \tag{12}$$

The maximum power-transfer condition is the first circulation adjustment. The second condition is obtained by magnetizing the junction. It is assumed throughout this paper that this condition is always readily obtained by the application of a suitable direct magnetic field. In one example studied in this text the experimental relation between the frequency responses of the demagnetized and magnetized junctions is shown in Fig. 4. It has a similar relation to that encountered in the case of stripline devices [12].

COUNTER-ROTATING JUNCTION MODES

It has recently been demonstrated that the waveguide-junction configuration used here supports axially resonating modes associated with the hybrid $HE_{1,1}$ unbounded dielectric waveguide mode [3], [4]. This section shows that the junction resonances are more precisely given by that of open dielectric resonators.

The result is given in Fig. 5 in the form of k_0R versus R/L. It applies to the single cylinder of length $2L$ and diameter $2R$ which is OC at both ends. It also applies to the disk L long, OC at one end and SC at the other. The boundary conditions are satisfied by first forming the field equations of the HE_{11} unbounded dielectric waveguide. Inside the dielectric region the longitudinal components of electric and magnetic fields are given by [19]

$$E_z = a_n{}^i J_n(kr) \exp(jn\theta) \tag{13}$$

$$H_z = b_n{}^i J_n(kr) \exp(jn\theta). \tag{14}$$

Outside the dielectric region the fields are

$$E_z = a_n{}^0 H_n{}^{(1)}(k_1 r) \exp(jn\theta) \tag{15}$$

$$H_z = b_n{}^0 H_n{}^{(1)}(k_1 r) \exp(jn\theta) \tag{16}$$

where J_n and H_n are Bessel's functions of the first and third kinds

$$k^2 = \frac{(2\pi\epsilon_r{}^{1/2})^2}{\lambda_0} - \left(\frac{2\pi}{\lambda_g}\right)^2 \tag{17}$$

$$k_1{}^2 = \left(\frac{2\pi}{\lambda_0}\right)^2 - \left(\frac{2\pi}{\lambda_g}\right)^2. \tag{18}$$

A factor of $\exp[j(\omega t - \beta z)]$ is omitted in the field equations.

The transverse components of the electric and magnetic fields for the inside and outside of the unbounded dielectric waveguide are given from Maxwell's equations in the usual way.

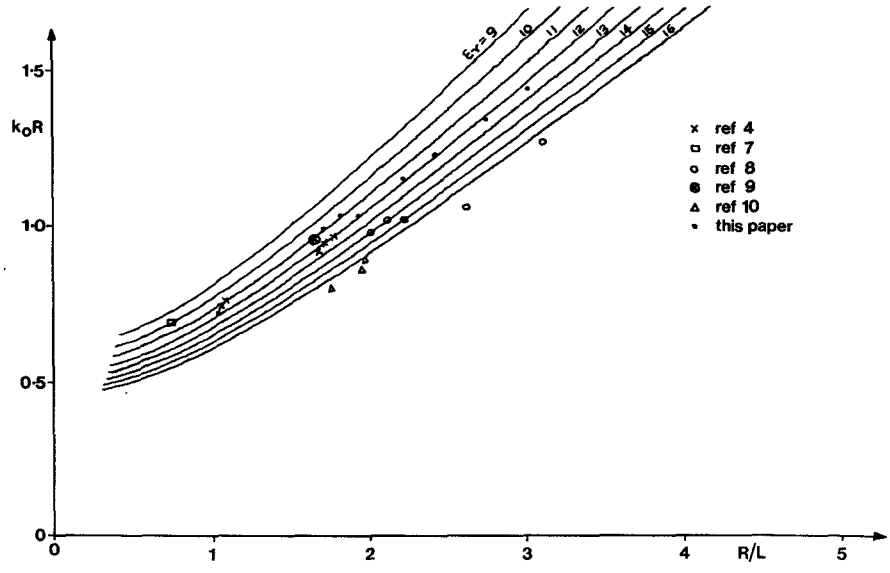

Fig. 5. Mode chart for open dielectric TM_{111} resonator.

Inside the dielectric region the result is

$$H_\theta = [r/(kr)^2]\{-j\omega\epsilon_r\epsilon_0(kr)a_n{}^iJ_n'(kr) + n\beta b_n{}^iJ_n(kr)\}\exp(jn\theta) \quad (19)$$

$$E_\theta = [r/(kr)^2]\{n\beta a_n{}^iJ_n(kr) + j\omega\mu_0(kr)b_n{}^iJ_n'(kr)\}\exp(jn\theta) \quad (20)$$

where

$$\beta = 2\pi/\lambda_g. \quad (21)$$

The boundary condition here is $s_1 = +1$ which coincides with

$$H_\theta = (\delta/\delta r)(rE_\theta) = 0. \quad (22)$$

This condition is satisfied provided

$$k_0R = (\epsilon_r)^{-1/2}\cdot n \quad (23)$$

$$b_n{}^i = J_n'(kR) = 0 \quad (24)$$

$$a_n{}^i = J_n(kR) = 0. \quad (25)$$

The first solution gives the radius at which $H_\theta = 0$ for the hybrid HE_{11} mode. The second and third equations represent TM and TE solutions. Since the radius associated with the hybrid solution is much smaller than that encountered in practice it is disregarded. For $n = 1$ the TM mode is the dominant one and its solution is found to be in good agreement with experiment. However, the TM solution adopted here does not exclude the possibility of operating partial-height ferrite circulators with hybrid HE_{11} mode for which $H_\theta \neq 0$.

The result is

$$J_n'(kR) = 0. \quad (26)$$

The solution is given by $(kR)n,j$ where n,j denotes jth root of the nth-order equation. For $n = 1$, the result is

$$(kR)_{1,1} = 1.84 = \left[\left(\frac{2\pi\epsilon_r{}^{1/2}}{\lambda_0}\right)^2 - \left(\frac{2\pi}{\lambda_g}\right)^2\right]^{1/2} R. \quad (27)$$

For a quarter-wave dielectric resonator with an electric wall at one face and a magnetic wall at the other

$$\lambda_g = 4L. \quad (28)$$

Combining the last two equations gives

$$(k_0R) = \frac{1}{\epsilon_r{}^{1/2}}\left[\left(\frac{\pi R}{2L}\right)^2 + (1.84)^2\right]^{1/2} \quad (29)$$

where

$$k_0 = 2\pi/\lambda_0. \quad (30)$$

Fig. 5 gives the mode chart for such an open dielectric resonator. It shows that the ferrite dimensions are not unique in that there is a wide choice of possible solutions which will establish the proper frequency with $H_\theta = 0$ at $r = R$. However, each shape will have its own Q factor.

Some experimental results obtained from the literature and in this work are superimposed on the mode chart for E plane, and both types of H-plane junctions suggest that they all use a TM_{11} open dielectric resonator mode.

It is useful to note that for large R/L, the resonant frequency of the ferrite disk is primarily dependent upon L which is determined from the gradient of the curve on the mode chart.

However, the introduction of the image plane or waveguide wall in the vicinity of the open dielectric resonator perturbs its resonant frequency. A suitable correction factor for the ferrite length is [16], [17]

$$\Delta L = \frac{1}{\beta}\tan^{-1}\left[\frac{\alpha\epsilon_r}{\beta}\tanh(\alpha s)\right] - L \quad (31)$$

where $\alpha = (k^2 - k_0{}^2)^{1/2}$. The spacing s is measured from the OC face of the ferrite to the image plane or waveguide wall depending on the geometry used.

CHARACTERISTIC PLANE OF H-PLANE JUNCTION

The characteristic planes in a 3-port junction coincide with those at which a short circuit placed in one port will cause a wave at the input port to be completely reflected, none entering the third one. These planes need not coincide with the terminals of the junction. Another property of these planes is that when a wave incident on the junction at one port is totally reflected by the location of a short circuit at a characteristic plane of a second port, the electric field vanishes at all characteristic planes in the other ones. This is the boundary condition used in this paper to determine the characteristic plane in the geometry considered here. A further property of characteristic planes is that the values of the admittance in each port extrapolated back to the characteristic plane in each port are related in a standard way. These properties are fully discussed in [5].

The purpose of this section is to give experimental and theoretical results on the characteristic plane of a 3-port symmetrical-waveguide junction loaded with a single or a pair of open dielectric resonators. This work shows that the characteristic plane of the junction fixes the input terminals of the radial impedance transformer.

The theory of the waveguide junction developed here starts by adjusting the terminals of the junction to make them coincide with those of the characteristic planes. It is assumed that an OC boundary condition exists at the surface of the ferrite region and that the $n = 1$ mode exists in the intermediate region. The boundary conditions used here transform an OC boundary condition at the terminals of the dielectric post to a SC one at the terminals of the waveguide. This perturbation of the junction is obtained when $s_1 = -1$ at $r = R_0$.

At $r = R_0$ the boundary condition is

$$E_z = 0 \tag{32}$$

for which

$$B_1 J_1(k_0 R_0) + C_1 Y_1(K_0 R_0) = 0. \tag{33}$$

The former condition establishes the characteristic plane of the junction.

At $r = R$ the boundary condition is given by

$$H_\theta = 0 \tag{34}$$

for which

$$B_1 J_1'(k_0 R) + C_1 Y_1'(k_0 R) = 0. \tag{35}$$

This condition coincides with an OC boundary condition at the ferrite.

Combining these two equations gives

$$\frac{Y_1'(k_0 R)}{J_1'(k_0 R)} = \frac{Y_1(k_0 R_0)}{J_1(k_0 R_0)}. \tag{36}$$

This last equation defines the characteristic plane of the H-plane symmetrical 3-port waveguide junction loaded with a resonant pair of open dielectric resonators. Fig. 6

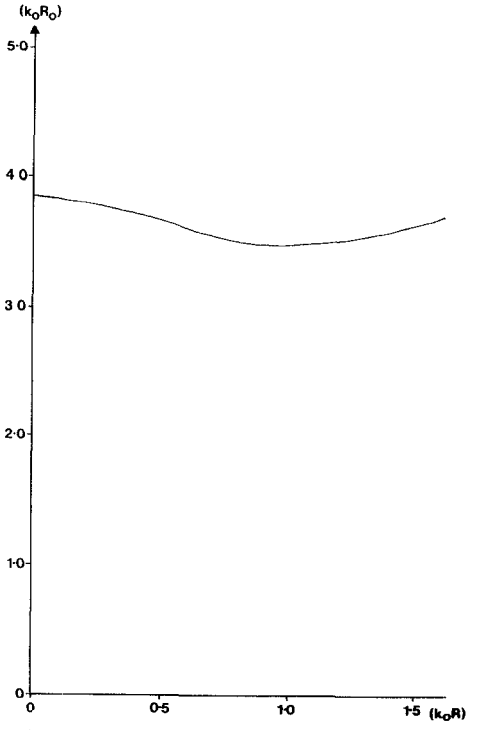

Fig. 6. Characteristic plane of H-plane waveguide junction.

gives the radial wavenumber k_0R_0 versus k_0R for such an arrangement. It shows, amongst other things, that the radial wavenumber is not strongly dependent upon k_0R.

The physical arrangement used to establish the characteristic plane of the waveguide junction is shown in Fig. 7(a). It consists of a 3-port waveguide junction with one port terminated by a short circuit at a radius r from the center of the junction. The characteristic plane is now obtained by measuring the position of the VSWR minimum at one of the ports with reference to the center of the junction with the other one terminated in a matched load. This is repeated for a number of different radii until the position of the VSWR minimum from the center of the device coincides with the radius of the junction. Fig. 7(b) gives a similar arrangement which applies to a straight junction.

Fig. 8 compares the characteristic plane for which $s_1 = -1$ with the plane at which $S_{11} = -1/3$. It shows that the characteristic plane may indeed be taken as the input terminals of the radial transformer.

IN-PHASE JUNCTION MODE

Maximum power transfer through the junction is the first circulation condition. It is met by adjusting the phase of s_0 with respect to s_1. The boundary condition on the TM_{01} mode is $s_0 = -1$ for which $E_z = 0$ at $r = R$, or $s_0 = +1$ for which $H_\theta = 0$ at $r = R_0$. The frequency variation of the in-phase mode has been measured by Owen also. This section describes a quasi-static approximation for it, which is consistent with these measurements.

In the quasi-static approximation employed here the partial-height geometry is replaced by a full-height one

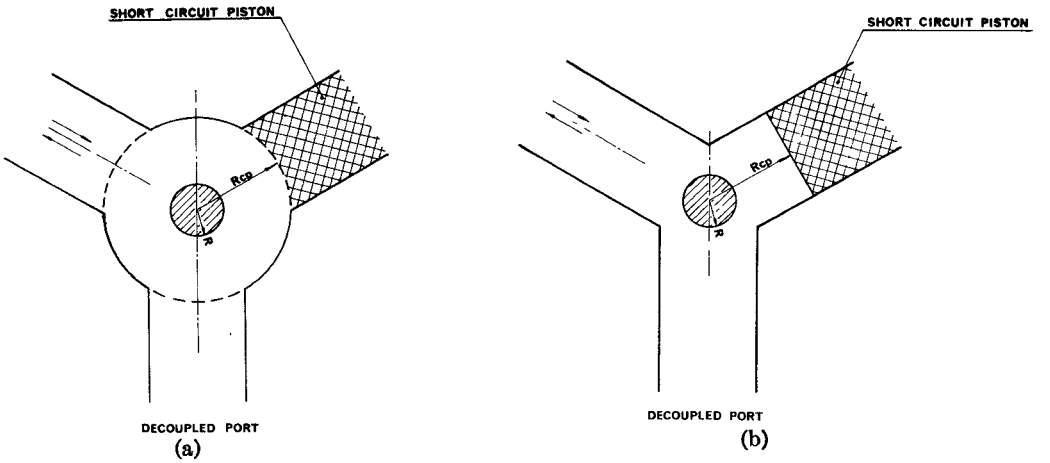

Fig. 7. (a) Method of measuring characteristic plane for circular junction. (b) Method of measuring characteristic plane for straight junction.

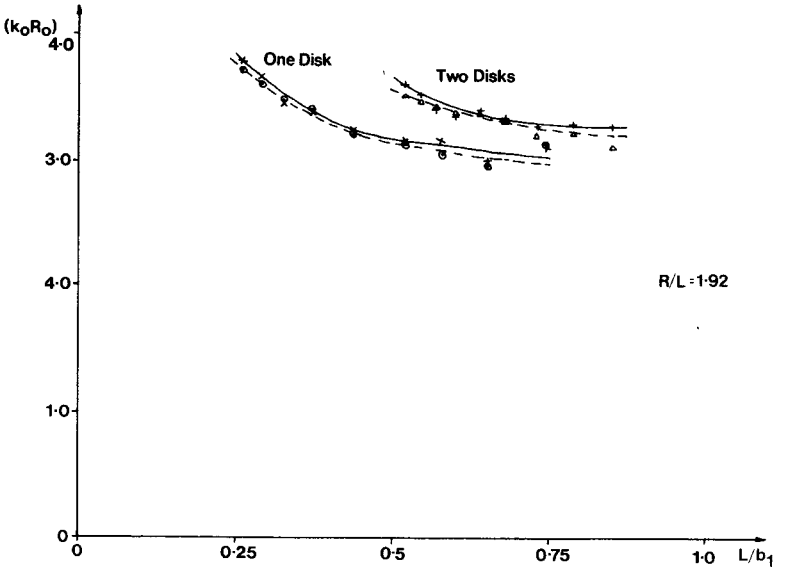

Fig. 8. Experimental characteristic plane at maximum power-transfer frequency.

with an equivalent quasi-static dielectric constant. A complete expansion for the fields inside and outside the bounded dielectric post for $n = 0$ is given in [13]. The asymptotic value of the reflection coefficient for the electric field using the asymptotic approximation for the Bessel's functions is therefore

$$s_0 = \exp(-j2\Phi_0) \tag{37}$$

where

$$\Phi_0 = (k_0 r + \tfrac{1}{4}\pi + \psi_0) \tag{38}$$

and ψ_0 is determined by equating the tangential components of E and H field at $r = R$.

$$\tan\psi_0 = \frac{\mu_e^{1/2} J_0(k_e R)\, Y_1(k_0 R) - \epsilon_e^{1/2} J_1(k_e R)\, Y_0(k_0 R)}{\epsilon_e^{1/2} J_0(k_0 R) J_1(k_e R) - \mu_e^{1/2} J_0(k_e R) J_1(k_0 R)} \tag{39}$$

where

$$k_e = k_0(\mu_e \epsilon_e)^{1/2} \tag{40}$$

$$\epsilon_e = \frac{\epsilon_r}{\epsilon_r - K(\epsilon_r - 1)} \tag{41}$$

$$\mu_e = 1 + K(\mu_d - 1) \tag{42}$$

$$K = L/b_1 \tag{43}$$

and μ_d is the demagnetized permeability.

Fig. 9 gives the phase angle of the in-phase mode as a function of $k_0 r$ for parametric values of L/b_1. This illustration allows L/b_1 to be determined at $k_0 R$ for which $s_0 = -1$ and at $k_0 R_0$ for which $s_0 = 1$. Since the radial line is nonuniform, these two boundary conditions cannot be simultaneously satisfied with a unique value of L/b_1, but instead they set upper and lower bounds on it. To investigate a suitable compromise a series of high-quality devices were constructed at 6 GHz with a VSWR of 1.07 over the 5.925–6.425-GHz band.[1] These results are superimposed on Fig. 9. This indicates that a suitable range

[1] Ferranti Ltd., Dundee, Scotland.

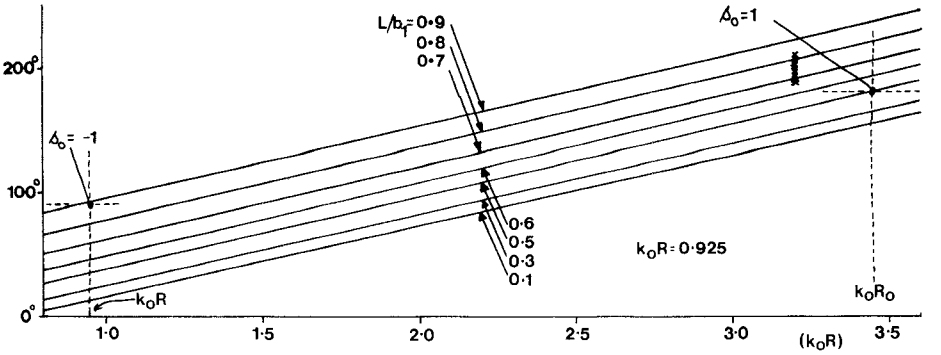

Fig. 9. Experimental and theoretical phase angle Φ_0 as a function of $k_0 r$.

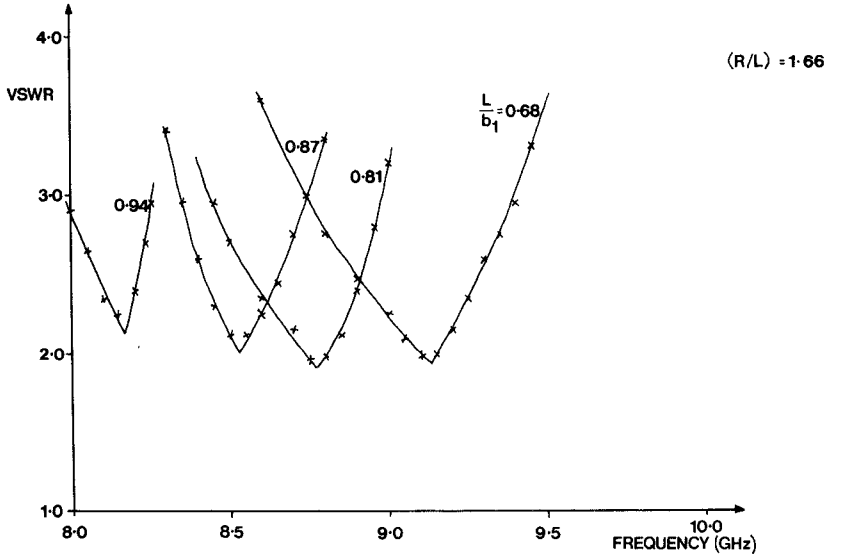

Fig. 10. Frequency response of reciprocal 3-port junctions.

for L/b_1 is 0.7–0.85 which in fact lies between the upper and lower limits of L/b_1 set by the boundary conditions.

EXPERIMENTAL SUSCEPTANCE-SLOPE PARAMETER OF JUNCTION

To obtain a 3-port circulator with an $n = 2$ Chebyshev frequency response it is necessary to establish the proper susceptance-slope parameter of the junction, which is determined by the turns ratio of the ideal transformers depicted in Fig. 3(a) and (b). Since no theoretical value is available, it must be obtained experimentally. The purpose of this section is to measure it as a function of L/b_1 for $R/L = 1.94$ and 1.67 for the geometries in Fig. 1(a)–(c). However, L/b_1 is essentially constrained by the phase angle of the in-phase eigenvalue to between 0.70–0.85, although it can be used as an independent variable to adjust the susceptance-slope parameter of the geometry in Fig. 1(c), provided the in-phase eigenvalue is tuned by a thin metal post.

One way the susceptance-slope parameters may be obtained experimentally is by measuring the frequency response of the demagnetized junction in the vicinity of the maximum power-transfer condition. In the structure studied each disk is mounted on a brass port which has the same diameter as the ferrite. The physical variables are the thickness of the disks and the spacing between them for disks having a fixed diameter of 10 mm.

Fig. 10 gives the frequency responses for one geometry studied in this paper. In Fig. 11 the mode charts of such transmission filters are constructed. These are solely determined by the dimensions of a single ferrite disk and its image plane in accordance with the transverse resonance condition [16], [17].

The dependence of the susceptance-slope parameter b' for the three junctions on the parameter L/b_1 is shown separately in Fig. 12. It is obtained from

$$b' = \frac{\frac{2}{3}[(r^2 - 2.5r + 1)/2r]^{1/2}}{2\delta} \tag{44}$$

provided the radial transformation is neglected, where r = VSWR and 2δ = normalized bandwidth.

The turns ratio of the ideal transformers may be calculated from the susceptance-slope parameter by assuming plane-wave propagation along the ferrite resonator. The result is

$$b' = a^2 \tfrac{1}{4}\pi \cdot (\epsilon_r/\mu_e)^{1/2}. \tag{45}$$

It is observed from these data that the first two geometries

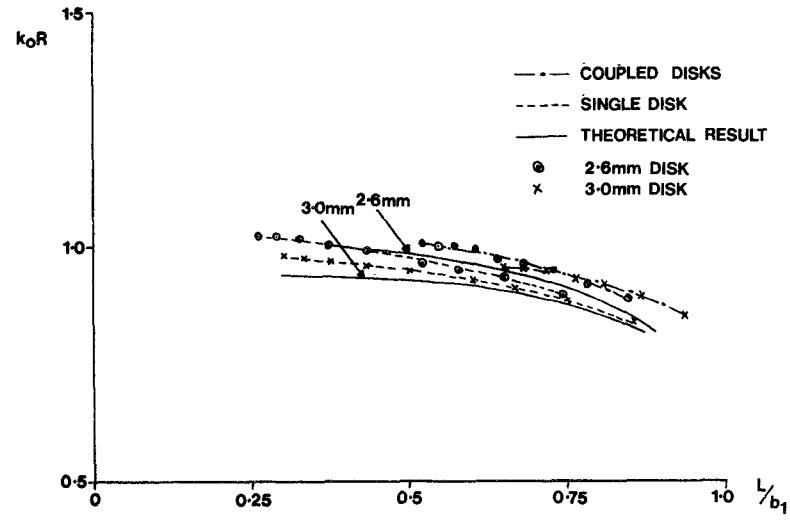

Fig. 11. Experimental mode chart for single and coupled TM_{111} resonators.

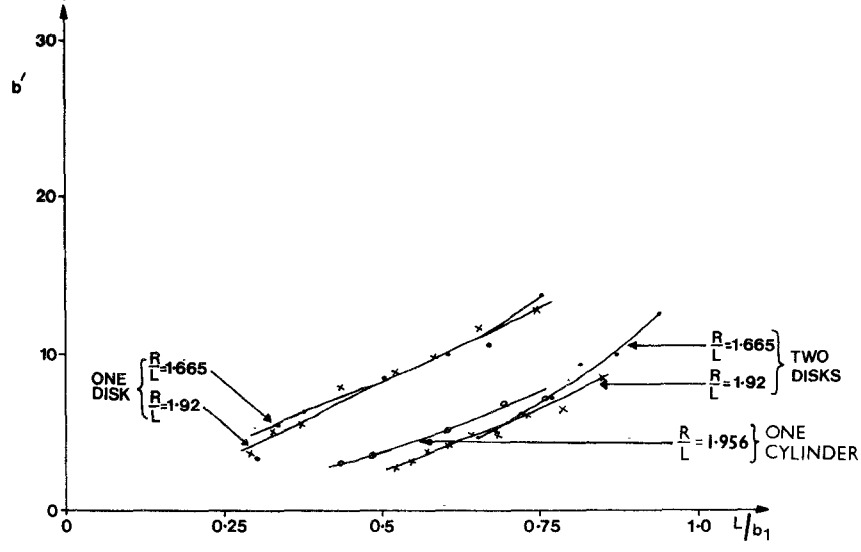

Fig. 12. Experimental susceptance-slope parameter of open dielectric resonators.

have identical susceptance-slope parameters while that of the third configuration is twice that of the other two. This suggests that the eigennetworks illustrated in Fig. 3(a) apply to the first two geometries while that depicted in Fig. 3(b) applies to the single-disk version. Since it has already been established by the method of images that the phase angles for all three geometries are the same, this further result suggests that provided all dimensions are measured with respect to the image planes, a single set of physical variables may be used to characterize all three circulator geometries. Since the three sets of eigennetworks are related, any one of them may be used to characterize the other two.

COUPLED FERRITE-DISK RADIAL WAVEGUIDE CIRCULATOR

The purpose of this section is to describe the experimental construction of a 3-port waveguide circulator with an $n = 2$ Chebyshev characteristic, using the configuration shown in Fig. 1(b). It consists of two circular ferrite disks in a radial cavity connected to three H-plane waveguides. In the construction used here the three rectangular waveguides are joined to the radial cavity at the characteristic planes of the junction. This latter condition therefore fixes the radius of the circular junction R_0. The radius R and the length L of the ferrite disks are determined by an open dielectric resonating $TM_{11\delta}$ mode. The values used in this text are $k_0R = 0.93$ and $R/L = 1.94$ [17]. For the two-disk geometry the susceptance-slope parameter of the junction, the phase angle of the in-phase eigennetwork, and the impedance of the radial nonuniform impedance transformer are all defined by L/b_1. The value of L/b_1 used here is determined from the section dealing with the in-phase mode. The design described is therefore defined by the following normalized quantities:

$$k_0R = 0.93$$

$$R/L = 1.94$$

$$k_cR_0 = 3.15$$

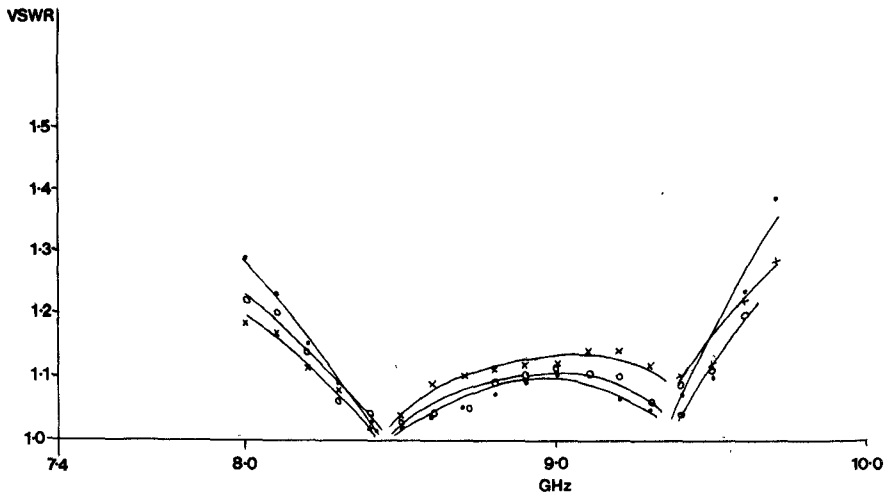

Fig. 13. Frequency response of two-resonator radial waveguide circulator.

$$L/b_1 = 0.77$$

$$2b_1/b = 0.59.$$

It should be noted that the radial wavenumber k_0R_0 is less than that of the theoretical value because of the step discontinuity associated with the radial transformer. Using a TT390 Ferrite material, the previously given quantities lead to the following linear dimensions for a junction at 9 GHz in the WR90 waveguide:

$$\lambda_0 = 33.3 \text{ mm}$$

$$R = 5.0 \text{ mm}$$

$$L = 2.3 \text{ mm } (2.60 \text{ mm})$$

$$R_0 = 16.7 \text{ mm}$$

$$2b_1 = 6.0 \text{ mm}$$

$$b = 10.16 \text{ mm}.$$

Fig. 13 shows the experimental frequency response for this device.

SINGLE FERRITE-DISK RADIAL WAVEGUIDE CIRCULATOR

This section describes the construction of the single ferrite waveguide circulator with an $n = 2$ Chebyshev characteristic. The configuration employed is shown in Fig. 1(c). It is obtained by establishing a 1:1 correspondence between the eigennetworks and the Q factors of the two junctions. The design described is defined by the following normalized quantities:

$$k_0R = 0.95$$

$$R/L = 1.92$$

$$k_0R_0 = 2.80$$

$$L/b_1 = 0.427$$

$$b_2/b = 0.60.$$

The value of L/b_1 used here satisfies the equivalence between the Q factors of the two junctions but does not satisfy the phase angles of the in-phase eigennetworks.

Using a TT390 ferrite leads to the following linear dimensions for the device at 9 GHz:

$$\lambda_0 = 33.3 \text{ mm}$$

$$R = 5.0 \text{ mm}$$

$$L = 2.4 \text{ mm } (2.60 \text{ mm})$$

$$R_0 = 14.00 \text{ mm}$$

$$b_1 = 4.72 \text{ mm}$$

$$b_2 = 6.096 \text{ mm}$$

$$b = 10.16 \text{ mm}.$$

Fig. 14 shows the frequency response of such a circulator. This result was obtained with some additional fine tuning in the form of a thin metal post through the center of the junction to compensate for the incorrect phase angle of the in-phase eigennetwork. The ferrite shape used in this section is that employed in the coupled resonator junction.

A similar frequency response has also been obtained without the aid of a thin metal post with $L/b_1 = 0.80$.

CONCLUSIONS

This paper has studied three radial waveguide circulators with $n = 2$ Chebyshev characteristics. The radial dimensions of the devices were obtained theoretically by evaluating the phase angles of the junction eigennetworks, while the admittance levels were established experimentally by using the 1-port approximation of the circulator. The characteristic plane of such junctions was defined and shown to coincide with the input terminals of the device. The eigennetworks of all three circulators may be described by a single set of physical variables.

It was also found that the new geometry[2] which relies on a single disk leads to a wider range of characteristics than is possible with the conventional coupled-disk version

[2] U.S. and U.K. patents filed.

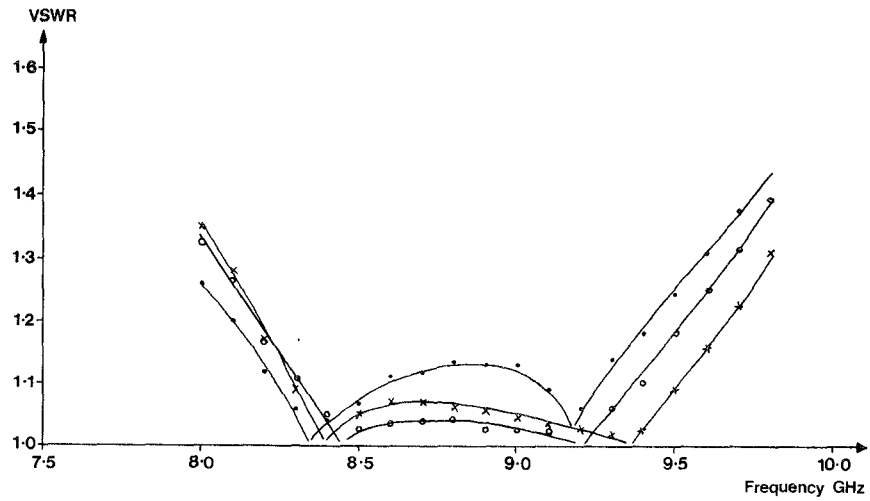

Fig. 14. Frequency response of single-resonator waveguide circulator.

where more than one electrical parameter is influenced by a single physical variable.

ACKNOWLEDGMENT

The authors wish to thank P. Cohen of Ferranti Ltd., Dundee, for many helpful discussions on image planes.

REFERENCES

[1] F. M. Aitken and R. McLean, "Some properties of the waveguide *Y* circulator," *Proc. Inst. Elec. Eng.*, vol. 110, Feb. 1963.
[2] B. Owen and C. E. Barnes, "The compact turnstile circulator," *IEEE Trans. Microwave Theory Tech. (1970 Symposium Issue)*, vol. MTT-18, pp. 1096–1100, Dec. 1970.
[3] J. Penny, "Experiments in the design of some three-port circulators," in *Proc. Inst. Elec. Eng. Conf. Microwave Circuits*, 1962.
[4] B. Owen, "The identification of modal resonances in ferrite loaded waveguide *Y*-junction and their adjustment for circulation," *Bell Syst. Tech. J.*, vol. 51, Mar. 1972.
[5] J. G. Allanson, R. Cooper, and Z. G. Cowling, "The theory and experimental behaviour of right-angled junctions in rectangular-section waveguides," *J. Inst. Elec. Eng.*, vol. 93, pt. III, pp. 177–187, 1949.
[6] B. A. Auld, "The synthesis of symmetrical waveguide circulators," *IRE Trans. Microwave Theory Tech.*, vol. MTT-7, pp. 238–246, Apr. 1959.
[7] M. Omori, "An improved *E*-plane waveguide circulator," in *G-MTT Int. Microwave Symp. Dig.*, 1968, p. 228.
[8] J. Helszajn and M. McDermott, "Mode chart for *E*-plane circulators," *IEEE Trans. Microwave Theory Tech.* (Corresp.), vol. MTT-20, pp. 187–188, Feb. 1972.
[9] J. Helszajn, "Waveguide and stripline 4-port single-junction circulators," *IEEE Trans. Microwave Theory Tech.* (Short Papers), vol. MTT-21, pp. 630–633, Oct. 1973.
[10] D. Burtt, Bell Northern Res., Ottawa, Ont., Canada, private communication.
[11] C. G. Montgomery, R. H. Dicke, and E. M. Purcell, *Principles of Microwave Circuits*. New York: McGraw-Hill, 1948.
[12] J. Helszajn, "Frequency response of quarter-wave coupled reciprocal stripline junctions, *IEEE Trans. Microwave Theory Tech.*, vol. MTT-21, pp. 533–537, Aug. 1973.
[13] J. B. Davies, "An analysis of the *m*-port symmetrical *H*-plane waveguide junction with central ferrite post," *IRE Trans. Microwave Theory Tech. (1962 Symposium Issue)*, vol. MTT-10, pp. 596–604, Nov. 1962.
[14] J. B. Castillo, Jr., and L. E. Davis, "Computer-aided design of three-port waveguide junction circulators," *IEEE Trans. Microwave Theory Tech.*, vol. MTT-18, pp. 25–34, Jan. 1970.
[15] J. Helszajn, "Scattering matrices of junction circulators with Chebyshev characteristics," submitted to *IEEE Trans. Microwave Theory Tech.*
[16] E. O. Ammann and R. J. Morris, "Tunable, dielectric-loaded microwave cavities capable of high *Q* and high filling factor," *IEEE Trans. Microwave Theory Tech.*, vol. MTT-11, pp. 528–542, Nov. 1963.
[17] J. Helszajn and F. C. F. Tan, "Mode charts for partial height ferrite waveguide circulators," *Proc. Inst. Elec. Eng.*, to be published.
[18] T. Schaug-Pattersen, "Novel design of a 3-port circulator," Norwegian Defence Res. Establ. Rep., Jan. 1958.
[19] P. J. B. Clarricoats, "Propagation along unbounded and bounded dielectric rods, Part 1 and 2," *Proc. Inst. Elec. Eng.*, vol. 108C, pp. 170 and 177, 1961.